A new method for high-energy pulsed Gamma measurement within intense background x-rays

Tan Xin-Jian(谭新建)[a)b)], Ouyang Xiao-Ping(欧阳晓平)[a)b)†], Wang Qun-Shu(王群书)[a)b)], Song Zhao-Hui(宋朝晖)[b)], Kang Ke-Jun(康克军)[a)], and Xia Liang-Bin(夏良斌)[b)]

[a)] *Department of Engineering Physics, Tsinghua University, Key Laboratory of Particle & Radiation Imaging (Tsinghua University), Ministry of Education, Beijing* 100084, *China*
[b)] *Northwest Institute of Nuclear Technology, Xi'an* 710024, *China*

(Received 3 May 2009; revised manuscript received 9 June 2009)

The accelerator-generating 6.13 MeV pulsed Gamma by ^{19}F(p, $\alpha\gamma$)^{16}O reaction usually synchronizes with an intense bremsstrahlung x-ray which has a maximum energy of 1 MeV. This paper proposes a new method, named the scattering and absorbing method, to diagnose the 6.13 MeV Gamma. This method includes two parts: the detector and a scatterer placed in front of the detector. The detector converts the Gamma to electrons and then collects the electrons by a scintillator. In order to restrain the interference of the low-energy background, the scintillator collects the electrons at a small angle. The scintillator is wrapped with electro-absorbing material to absorb the low-energy electrons generated by background x-rays. The theoretical sensitivity ratio of 6.13 MeV Gamma to 1 MeV x-rays is greater than 150. The scatterer is a pretreatment tool to scatter some background x-rays away from the radial beam before they enter the detector. By varying the length, the scatterer can reduce the background x-rays to an acceptable level for the detector.

Keywords: high energy pulsed Gamma, background, scattering, absorbing
PACC: 0785, 2940M, 2990

1. Introduction

In the field of pulsed radiation detecting,[1] intense background is unavoidable, sometimes crucial. For example, the 16.7 MeV Gamma from the Deuterium–Tritium (D–T) reaction has been used to diagnose the weapon at the Nevada Test Site (NTS). But the lower energy Gamma (2 MeV on average) background flux is expected to be several orders of magnitude larger than the peak flux of 16.7 MeV Gamma.[2] Moreover, pulsed Gamma generated by an accelerator from a (p, γ) resonant reaction is useful as an important radiation source for detector calibration. However, the bremsstrahlung x-ray background is intense. In the ^{19}F(p,$\alpha\gamma$)^{16}O reaction, the bremsstrahlung x-ray (with a maximum energy of 1 MeV and an average of 0.67 MeV) background flux is more than one order of magnitude larger than the 6.13 MeV Gamma[3].

As the energy of background Gamma (or x-rays) is much lower than that of the aimed Gamma, threshold Gamma detectors which are only sensitive to some specified energy range are required. Los Alamos National Laboratory (LANL), Lawrence Livermore National Laboratory (LLNL) and Chinese Academy of Engineering Physics (CAEP) have developed diagnostic systems[4,5] for the measurement of the reaction time history of the D–T burn. Such systems have provided a high signal-to-noise ratio (about $10^5 - 10^6$). However, because of the low sensitivity, it is hard to extend this system to other applications such as accelerator-generating pulsed Gamma.

In this paper, a new method to measure high energy pulsed Gamma from intense lower-energy Gamma (or x-ray) background, named the 'Scattering and Absorbing Method' (SAM for short), is proposed and a detector for the application of 6.13 MeV pulsed Gamma measurement has been designed.

2. SAM method

The SAM method consists of two parts: the detector and the scatterer. The scatterer will be introduced later as an enhanced version.

Figure 1 illustrates the structure of the SAM detector. The detector first converts a Gamma to an electron (or positron) and then collects scintillation light induced by the electron (or positron).

†Corresponding author. E-mail: oyxp2003@yahoo.com.cn
© 2010 Chinese Physical Society and IOP Publishing Ltd

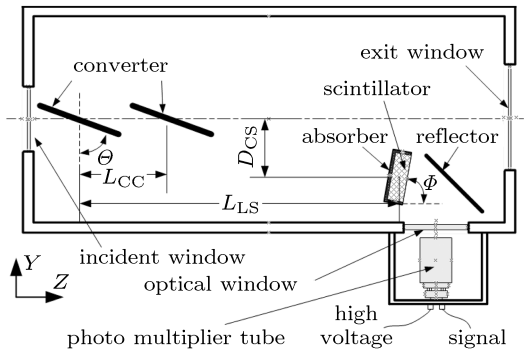


Fig. 1. Schematic diagram of the SAM detector. Two separate converters are used to increase the transforming efficiency. The scintillator detects the secondary electrons or positrons generated by the converter and the reflector reflects the scintillation light through the optical widow, where the light signal will be recorded by an optical device such as a Photo Multiplier Tube (PMT). The absorber material absorbs the secondary electron generated by background x-rays.

At the energies relevant to this diagnosis, Gamma-to-electron conversion is accomplished by Compton scattering and pair production.

In Compton scattering, the incident Gamma photon is deflected through an angle θ with respect to its original direction, and transfers a portion of its energy to the recoil electron which ejects through an angle ϕ with regard to the original Gamma direction. The angles θ and ϕ obey the following equation in the case of ignoring the binding energy of the recoil electron:

$$\cot\phi = (1+\alpha)\mathrm{tg}\,(\theta/2), \tag{1}$$

where $\alpha \equiv h\nu/m_0c^2$. The angular distribution of scattered Gammas is predicted by the Klein–Nishina formula[6] for the differential scattering cross section:

$$\frac{\mathrm{d}\sigma}{\mathrm{d}\Omega} = Zr_0^2\left(\frac{1}{1+\alpha(1-\cos\theta)}\right)^2\left(\frac{1+\cos^2\theta}{2}\right) \times\left(1+\frac{\alpha^2(1-\cos\theta)^2}{(1+\cos^2\theta)[1+\alpha(1-\cos\theta)]}\right), \tag{2}$$

where Z is the atomic number of the material, and r_0 is the classical electron radius. According to formulas (1) and (2), Table 1 gives the angle $\theta_{\max}$ and angle $\phi_{\max}$, at which the emitting probability is maximum for scattered Gamma and the recoil-electron respectively. Obviously, the $\phi_{\max}$ of 6.13 MeV Gamma is much smaller than that of 0.67 MeV and 1 MeV Gamma.

Table 1. The peak position of angle distribution for scattered Gamma and the recoil electron.

$h\nu$/MeV	0.67	1.00	6.13
$\theta_{\max}/(^\circ)$	32.6	29.0	14.5
$\phi_{\max}/(^\circ)$	16.3	13.5	3.9

Pair production occurs only when the Gamma energy exceeds 1.02 MeV, which is equal to twice the rest-mass energy of an electron. Suppose the secondary electron (or positron) with kinetic energy T_{e}' emits through an angle β with respect to the incident Gamma direction. The following formula shows the mean square root of angle β.[7]

$$\left\langle\beta^2\right\rangle^{1/2} = q'(h\nu, T_{\mathrm{e}}', Z)\left(\frac{m_0c^2}{h\nu}\right)\ln\left(\frac{h\nu}{m_0c^2}\right), \tag{3}$$

where q' is the function of atomic number Z, $h\nu$ and T_{e}'. Function q' almost always equals one. For 6.13 MeV Gamma, formula (3) could be rewritten as formula (4).

$$\left\langle\beta^2\right\rangle^{1/2} = 0.207q'(6.13\ \mathrm{MeV}, T_{\mathrm{e}}', Z) \approx 11.9^\circ. \tag{4}$$

In a word, most of the secondary electrons (or positrons) generated by 6.13 MeV Gamma emit through a relatively small angle with regard to the incident Gamma original direction. However, as a result of multiple Coulomb scattering, the emitting angle will be enlarged, and the angle distribution will be broadened. The optimum mass thickness of a tungsten (W) converter is 0.12 g/cm^2, at which the peak emitting angle of the secondary electron (or positron) is about 11 degrees (see Fig. 2). The scintillator detects the secondary electron (or positron) at this angle too. A thinner converter will reduce the secondary electron detecting angle, which will require the Gamma to be much better collimated. A thicker converter will increase the interference of secondary photons generated by the background x-rays.

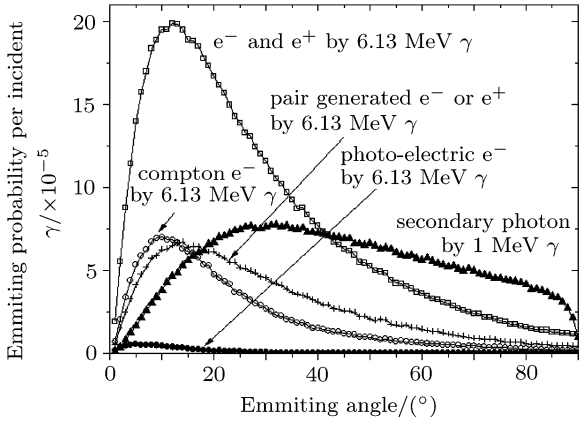


Fig. 2. The angular distribution of secondary electron and positron converted from 6.13 MeV Gamma by W with mass thickness of 0.12 g/cm^2.

According to Fig. 2, the proper angle to detect secondary electrons is $7^\circ - 15^\circ$. Figure 3 illustrates the energy spectrum of electrons emitted in that angle. The energy of most of the electrons generated by 6.13 MeV Gamma is much higher than that by 1 MeV or 0.5 MeV background x-rays. The electron generated by background x-rays will be readily absorbed when transported in absorbing material. Meanwhile, the electron generated by 6.13 MeV Gamma will not be affected except for some energy loss. As is shown in Fig. 4, only about 2 percentages energy of a 1 MeV electron could pass through 4 millimeters polythene ($(CH_2)_n$, PE for short) while it is more than 70 percentages for an electron with energy greater than 3 MeV.

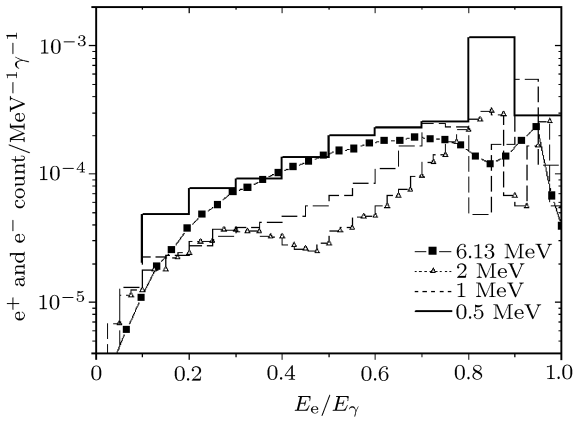


Fig. 3. Energy spectrum of electrons emitted between 7° to 15°.

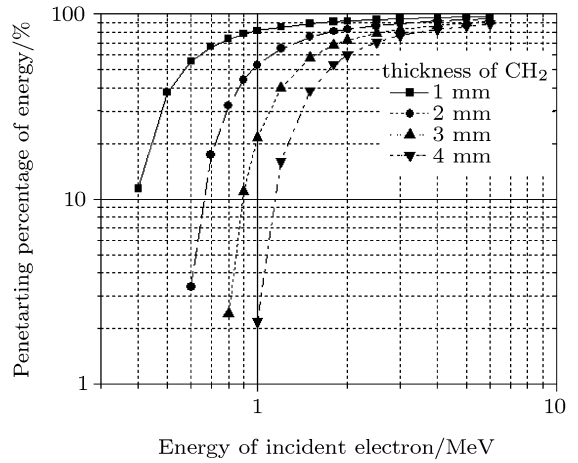


Fig. 4. The energy percentage of an electron that penetrates 1–4 mm PE.

3. Monte Carlo simulation

A simulation code based on Geant4[8] has been developed to track the time and spatial history of an electron (positron) generated by 0.5–6.13 MeV Gamma. To optimize the converter thickness and scintillator detecting angle, the code records the angular spectra of the secondary electron (positron) and scattered Gamma (see Fig. 2 and 3). To get the largest sensitivity ratio (K) for 6.13 MeV to 1 MeV Gamma, the sensitivity of detectors with scintillators and absorbers (PE) of varying thickness has been studied.

The final detector structures after optimization are as follows. Two tungsten (W) converters (30 mm× 30 mm × 0.0213 mm, $\rho = 19.3$ g/cm^3) with rotation angle 70° (Θ), central distance (L_{CC}) 30 mm. The scintillator material is ST401 (80 mm×8 mm×20 mm, $\rho = 1.05$ g/cm^3) with a rotating angle (Φ) of 80°. The central distances between the scintillator and the front converter along axes Y and Z are 32 mm (D_{CS}) and 164 mm (L_{CS}) respectively. All the scintillator surfaces except the posterior one (relative to the converter) are covered with absorber (4 mm PE, $\rho = 0.92$ g/cm^3).

The final sensitivity ratio K is larger than 150, according to the detector response curve to the incident Gamma (Fig. 5). Figure 6 illustrates the time history

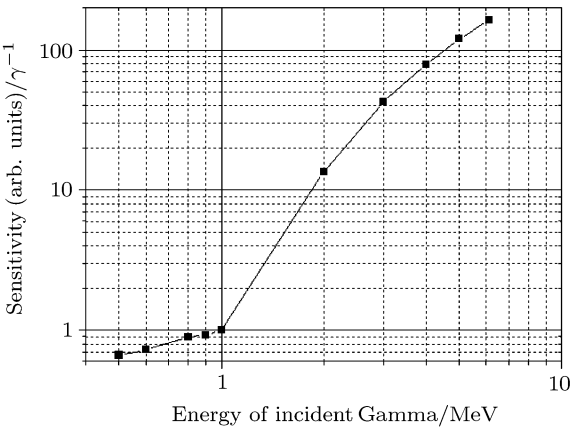


Fig. 5. The detector response curve to the incident Gamma energy.

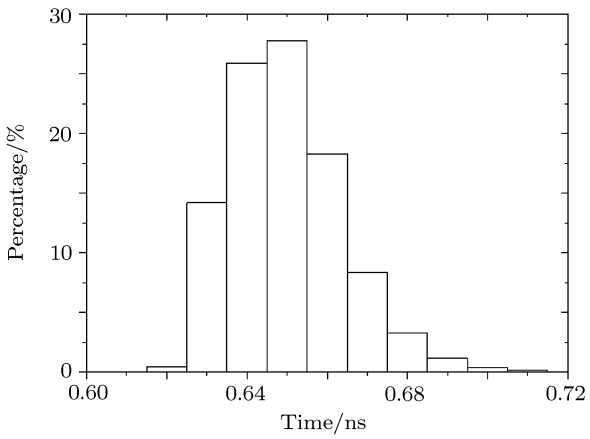


Fig. 6. Time history of energy deposition by 6.13 MeV Gamma.

of energy deposition by 6.13 MeV Gamma. All of the energy deposition is accomplished within 0.1 ns. Considering the decay constant for ST401 (2.4 ns [9]), the theoretical time resolution of the detector (neglecting the PMT) is approximately 2.4 ns.

4. Experiment proof

The sensitivity of the SAM detector has been studied with 6.13 MeV Gamma generated by the China Institute of Atomic Energy (CIAE) 600 keV Cockcroft–Walton accelerator. As the yield of the 6.13 MeV Gamma is just about $10^7 - 10^8\gamma$/s, the charge analog digital conversion technique[10] is used to calibrate the detector sensitivity.

As described above, the designed optimum thickness of the converters is 0.0213 mm. But this thickness is not accessible. So, we replaced it with a standard thickness (0.08 mm). Simultaneously, the related parameters are set as follows to collect the secondary electrons generated by 6.13 MeV Gamma: Θ (55°) , $D_{\rm CS}$ (31.5 mm) and $L_{\rm CS}$ (142 mm).

Figure 7 illustrates the simulated energy deposition spectrum and the measured pulsed charge spectrum. These two spectra match pretty well in the shape.

In order to prove that the detector is not sensitive to the low-energy Gamma (or x-ray), the sensitivity for the 1.25 MeV Gamma, which is generated by a ^{60}Co source, has also been measured.

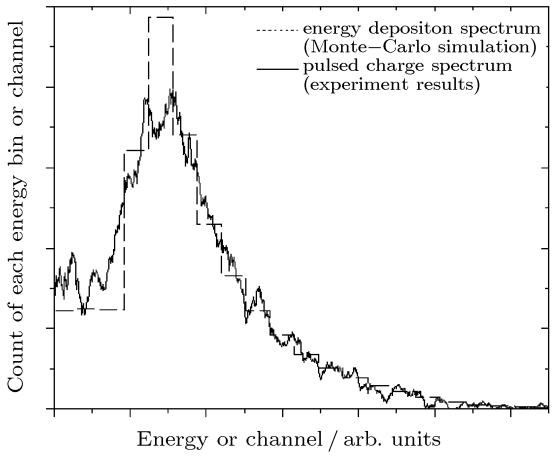


Fig. 7. The simulated energy deposition spectrum and measured pulsed charged spectrum by 6.13 MeV Gamma.

Table 2 gives the simulated and measured detector sensitivity and detecting efficiency. The measured detecting efficiency is 1.24×10^{-3}. It matches the simulated result within 3.99% difference. The detector sensitivity to the 6.13 MeV Gamma is 2.20×10^{-14} C·cm^2. Moreover, the measured and simulated sensitivity ratio of 6.13 MeV to 1.25 MeV Gamma is 71.0 and 82.5 respectively.

Table 2. The detector's detecting efficiency and sensitivity.

	detecting efficiency	sensitivity/C·cm^2		sensitivity ratio of 6.13 MeV to 1.25 MeV Gamma
E_γ/ MeV	6.13	6.13	1.25	
simulated value	1.29×10^{-3}	–	–	82.5
measured value	1.24×10^{-3}	2.20×10^{-14}	3.12×10^{-16}	71.0
difference	3.99%	–	–	14.0%

The experiment results demonstrate that the SAM detector has a large sensitivity ratio of 6.13 MeV Gamma to low energy photons.

5. Enhanced version

An enhanced version has been designed to handle the situation in which the background x-ray is much more intense.

A scatterer is placed in front of the detector. This means that the radial-rays which enter the detector through the entrance window have to pass through the scatterer first.

The scatterer is some specific media that would scatter many more Background Photons (BP, Gamma or x-ray), relative to the Aimed Gamma (AG), away from the original beam direction. Suppose that the original particle fluence for AG and BP is $\varphi_{\rm H1}$ and $\varphi_{\rm L1}$, and the attenuated fluence is $\varphi_{\rm H2}$ and $\varphi_{\rm L2}$, respectively, after vertically penetrating a scatterer with thickness l. The AG and BP separating ability is defined as $P(l)$:

$$P(l) \equiv \frac{\varphi_{H2}/\varphi_{L2}}{\varphi_{H1}/\varphi_{L1}} = \frac{\varphi_{H2}/\varphi_{H1}}{\varphi_{L2}/\varphi_{L1}} = \frac{P_H(l)}{P_L(l)} = \exp((\Sigma_L - \Sigma_H) \times l) = \exp(\mu_{HL} l), \quad (5)$$

where $P_H(l)$ and $P_L(l)$ are the penetrating probabilities for AG and BP, Σ_H and Σ_L are the macro cross sections for AG and BP in the scatter medium. $\mu_{HL} \equiv \Sigma_L - \Sigma_H$. When μ_{HL} is larger than zero, the BP will attenuate faster than AG.

It is apparent that the AG should penetrate the medium as much as possible. Formula (5) can be rewritten as:

$$P_H(l) = P(l)^{-\frac{\Sigma_H}{\Sigma_L - \Sigma_H}} \equiv P(l)^{-\varepsilon_{HL}}, \quad (6)$$

where $\varepsilon_{HL} \equiv \Sigma_H/(\Sigma_L - \Sigma_H)$. It is obvious that the smaller the ε_{HL}, the more the penetrating AG is.

The attenuating multiple of the AG ($\phi_{H1}/\phi_{H2} = 1/P_H(l)$) represents the cost to achieve the separating ability $P(l)$. Define $\zeta(l) \equiv P(l)/(\varphi_{H1}/\varphi_{H2})$, which stands for the separating ability acquired by each attenuating multiple of the AG.

$$\zeta(l) \equiv \frac{P(l)}{\varphi_{H1}/\varphi_{H2}} = \exp((\Sigma_L - 2\Sigma_H) l) = \exp(\eta_{HL} l), \quad (7)$$

where $\eta_{HL} \equiv \Sigma_L - 2\Sigma_H$. It is obvious that the bigger the η_{HL} is, the easier it is to separate AG and BP at the same cost.

The values of μ_{HL}, ε_{HL} and $\eta_{HL}$for some common media are given by Table 3. Graphite (C), whose η_{HL} is the biggest among the listed media, is the best scatterer for 6.13 MeV AG and 1 MeV BP.

Table 3. The values of μ_{HL}, ε_{HL} and η_{HL} for some media (for 6.13 MeV and 1 MeV).

medium	density/(g/cm^3)	μ_{HL}	ε_{HL}	η_{HL}
PE	0.92	4.18×10^{-2}	7.49×10^{-1}	1.67×10^{-2}
C	2.62	1.03×10^{-1}	1.08	3.89×10^{-2}
Al	2.7	9.47×10^{-2}	6.00×10^{-1}	2.38×10^{-2}
Fe	7.86	2.31×10^{-1}	1.03	-7.59×10^{-3}
Ni	8.9	2.63×10^{-1}	6.21×10^{-1}	-2.15×10^{-2}
Pb	11.4	3.04×10^{-1}	1.65	-1.98×10^{-1}

The above deduction is based on the hypothesis that the scattered Gamma will not affect the detector. However, this hypothesis is not tenable for the scattered Gamma with small scattering angle. According to the simulation based on MCNP,[11] Fig. 8 illustrates the separating ability for graphite of varying length, where the φ_{H2}, φ_{L2}in formula (5) consists of the scattered Gamma between angle 0° and 10°. In reality, the length of the graphite should be chosen not only according to Fig. 8 but the intensity of the background relative to 6.13 MeV Gamma.

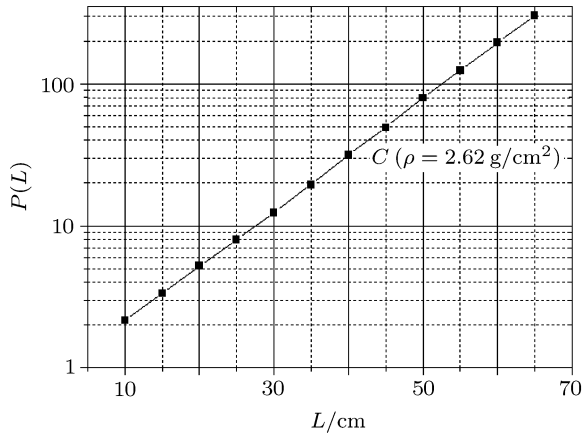


Fig. 8. The separating ability of graphite for 6.13 MeV and 1 MeV Gamma.

Figure 9 is the energy spectrum of the Gamma emitted between angle 0° and 10° when 6.13 MeV Gamma is penetrating 30 or 60 cm graphite. The scattered Gamma accounts for about 10% of the total emitting Gamma, and their energies concentrate within the range of 0–1.5 MeV and 5–6 MeV.

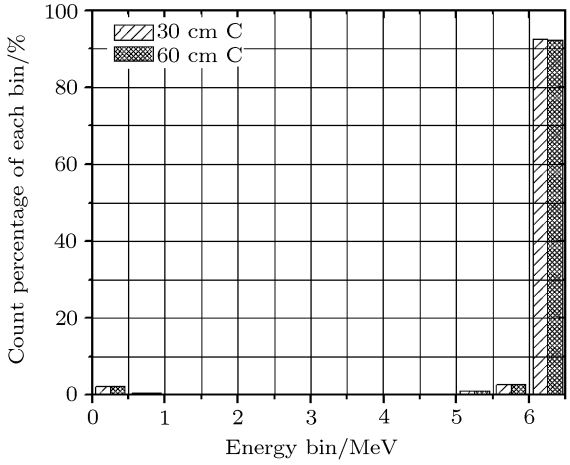


Fig. 9. The energy spectrum of the Gamma emitted between angle 0° and 10° by 6.13 MeV Gamma.

6. Discussion

Based on the fact that low-energy photons can be more attenuated in low-Z material and the distinct angular and energy distribution of secondary electrons between low-energy and high-energy photons, the SCAB method employs a specific detector arrangement to maximize the separation of Gamma rays from the low-energy x-ray background. Even if

in the extreme situation with an intense x-ray background, the detector is capable of reducing the background to an acceptable level.

The structure of SCAB the detector is simple and can be easily applied to high-energy pulsed Gamma ray detection. Moreover, the SCAB can handle different x-ray (Gamma) background levels by varying the length of the scatterer. For instance, using 35 cm graphite as the scatterer, the detector is able to achieve a signal-to-noise ratio as high as 3000 for a 6.13-MeV Gamma-ray pulse. If the scintillator ST401 and PMT are replaced with quicker units, such as scintillator BC422Q and a photoelectric tube, the SCAB can achieve subnanosecond time resolution. This also suggests that the SCAB has the potential to be extended to D–T fusion diagnosis.

References

[1] Xia L B, Ouyang X P, Wang Q S, Kang K J and Tan X J 2008 *Chin. Phys.* B **17** 4466

[2] John E B, Joseph S L, Peter B L, Joseph M M, James W T and Carlton S Y 1983 LA-UR-83-1864

[3] Yang H L and Qiu A C 2004 *Nuclear Techniques* **27** 188 (in Chinese)

[4] Berggren R R, Caldwell S E, Faulkner J R, Lerche R A, Mack J M, Moy K J, Oertel J A and Young C S 2001 *Rev. Sci. Instrum.* **72** 873

[5] Ye Y Y, Chen H D, He X J, Teng J T, Zhang C F, Feng J N, Chen X D and Deng F S 1996 *Atomic Energy Science and Technology* **30** 127 (in Chinese)

[6] Glenn F K 1999 *Radiation Detection and Measurement* (New York: John Wiley & Sons, Inc.) p51

[7] Xie Y G and Chen C 2003 *Particle Detector and Data Acquisition* (Beijing: Science) p23 (in Chinese)

[8] Agostinelli S 2003 *Nucl. Instrum. Methods* A **506** 250

[9] Guo Q, Xu R K and Lee Z H 2004 *Acta Phys. Sin.* **53** 1334 (in Chinese)

[10] Song Z H, Ruan X C, Dai Q S and Wang K L 2005 *High Power Laser and Particle Beams* **17** 453 (in Chinese)

[11] Briesmeister J F 2003 *MCNP-A General Monte Carlo N-particle Transport Code*, Version 5 (Alamos: National Laboratory)